

Wind Fragility Assessment for Roof Panel of Steel Framed Building

Gibae Kim*, Youngsun Choun, Gilyoung Chung, Soohyuk Chang
CENITS Corporation Inc., 233, Gasan digital 1-ro, Geumcheon-gu, Seoul, South Korea
*Corresponding author: kibae2@naver.com

***Keywords** : extreme wind, fragility assessment, monte carlo simulation, turbine building, roof panel

1. Introduction

The turbine building of a Nuclear Power Plant (NPP) is a steel framed structure with exterior panels installed. Exterior panels can be vulnerable to natural hazards. In particular, structural damage and failure are frequently caused by extreme winds, and the intensity of typhoons accompanied by extreme winds is increasing [1]. According to the stress test performance report in NPP [2], it is stated that damage such as failure of roof panels may occur due to extreme winds. This can lead to a serious accident if an extreme natural hazard that greatly exceeds the design standard occurs. In this study, a wind fragility assessment of the turbine building was performed assuming structural specifications to predict failures due to extreme winds. As an evaluation method, the Monte Carlo simulation algorithm of an analytical approach was applied.

2. Assessment Method

The wind fragility assessment for extreme winds samples a stochastic specimen considering uncertainty and repeatedly compares the limit state equation using Equation 1.

$$G(R, W) = R - W \quad (1)$$

Here, R is resistance performance, W is wind load.

2.1 Target Structure

A turbine building in NPP was selected as the target structure. The shape is the same as the turbine building, but the specifications of the exterior panels may differ from the actual one. As the major failure mode of the turbine building due to extreme winds was identified as roof panel failure [3], the wind fragility assessment of the roof panel was performed in this study. For turbine building, the length of the ridge parallel to the ridge is 96.0m, the length perpendicular to the ridge is 40.0m, and the height from the ground is 34.0m. The specifications of the panel were 2m wide, 4m long, steel skin 0.5t, thickness 100mm, and slope 2°. In addition, the external pressure coefficient of the roof panel was divided into three zones with reference to ASCE 7-16[4]. There are 352 units in zone 1, 104 units in zone 2, and 24 units in zone 3, for a total of 480 units, as shown in Fig. 1. For the resistance performance R of the roof panel, the value obtained through the pressure chamber test by

Baskaran et al. was applied [5]. The population mean is 3.25 kPa, and the Coefficient of Variation (COV) is 0.24.

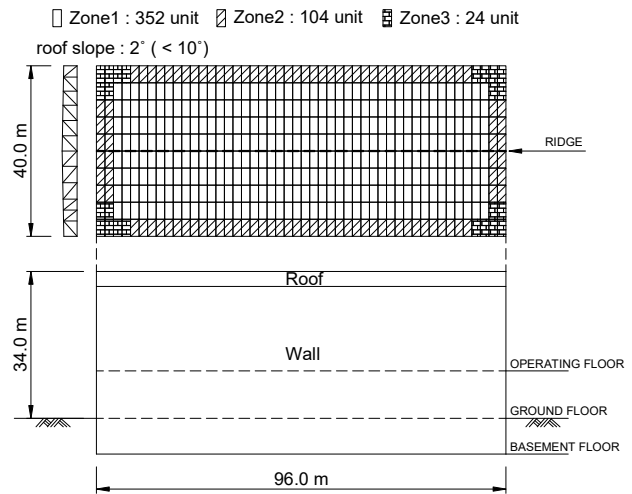


Fig. 1. Placement of Roof Panels

2.2 Wind Load

Equation 2 of part 3 ($h > 18m$) in components and cladding (chapter. 30) presented in ASCE 7-16 [4] was applied to the wind load calculation formula.

$$W = q(GC_p) - q_i(GC_{pi})(N/m^2) \quad (2)$$

Here, q is velocity pressure, GC_p is the product of the gust effect factor and the external pressure coefficient, and, GC_{pi} is the product of the gust effect factor and the internal pressure coefficient. Velocity pressure q follows Equation 3.

$$q = 0.613K_zK_{zt}K_dK_eV^2(N/m^2) \quad (3)$$

Here, K_z is velocity pressure exposure coefficient, K_{zt} is topographic factor, K_d is wind directionality factor, K_e is ground elevation factor, and V is wind velocity. These statistical parameters are shown in Table I [6, 7].

2.3 Monte Carlo Simulation of Analytical Approach

The wind fragility assessment can be approached by expert, empirical, analytical, and hybrid methods. In this study, an analytical method was applied, among which

Monte Carlo Simulation (MCS) algorithm was applied [8]. The MCS procedure is as follows. First, a specimen is sampled from a normal distribution (Fig. 2) and then an initial calculation is performed according to Equation 1. At this time, if the initial failure of the panel occurs, recalculation is performed assuming that internal pressure increases. This process is repeated 10,000 times for each wind velocity. The wind velocity was increased from 1 m/s to 80 m/s. This MCS algorithm is shown in Fig. 3.

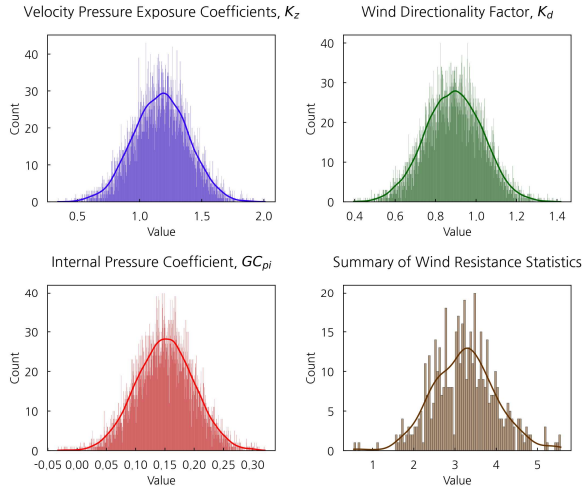


Fig. 2. Statistics of Parameters

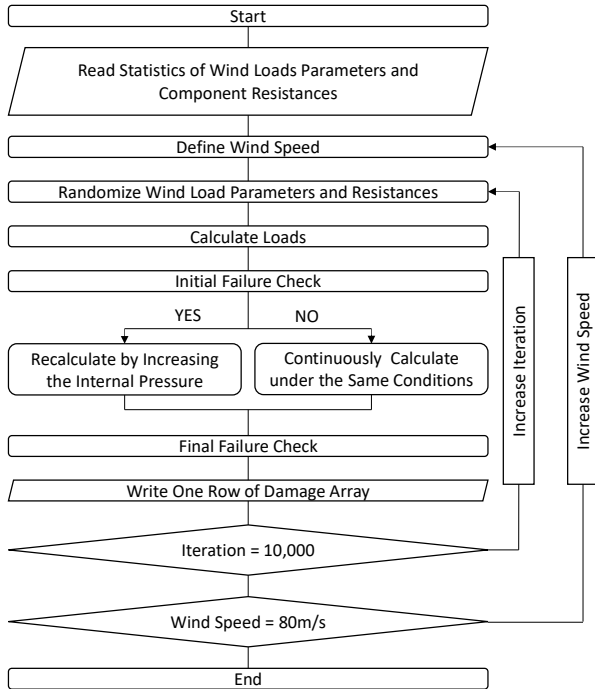


Fig. 3. Algorithm of the Monte Carlo Simulation

Table I: Statistics of Wind Load Parameters

Wind Parameter	Categories	Nominal	Mean	COV
K_z	Exposure B (0~53m)	1.15	1.17	0.19
	Exposure C (9.1~63m)	1.42	1.36	0.14
	Exposure D (6.1~63m)	1.57	1.52	0.14
K_d	Components & Cladding	0.85	0.89	0.16
GC_{pi}	Enclosed	0.18	0.15	0.33
	Partially enclosed	0.55	0.46	0.33
K_{zt}	1.00 (Deterministic)			
K_e	1.00 (Deterministic)			

2.4 Fragility Curve

By applying the MCS algorithm, the probability of failure for each wind velocity can be evaluated in the form of a discrete function. This needs to be converted to a continuous function to evaluate the probability of failure for arbitrary wind velocities, which can be converted in the form of a lognormal cumulative distribution using Equation 4 [9].

$$F_r(y) = \Phi \left[\frac{\ln(y) - m_R}{\xi_R} \right] \quad (4)$$

Here, Φ is the standard normal distribution function, m_R is the logarithmic median of capacity, ξ_R is the logarithmic standard deviation of capacity. To optimize the lognormal cumulative distribution function, the least square method was applied using in Equation 5.

$$\widehat{m}_R, \widehat{\xi}_R = \min \sum_{x=1}^n [P_f(v) - F_r(v)]^2 \quad (5)$$

Here, $P_f(v)$ is the failure probability of the roof panel evaluated by the MCSE algorithm, and $F_r(v)$ is the wind fragility of the exceedance failure probability optimized by the least squares method.

3. Analysis Results

The wind fragility assessment was performed by applying the MCS algorithm. Fig. 4 shows the comparison of the direction parallel to the ridge and the perpendicular direction to the ridge, and it was found that the effect on the wind direction was not significant. Since this is a flat roof with a roof slope of less than 10° , it is judged that there is no significant effect by applying the same external pressure coefficient as when the wind direction is perpendicular to the ridge. Fig. 5 shows the comparison of the exposure type, and it was confirmed that there is an effect depending on the exposure type where the structure is located. As a result of confirming the wind velocity that causes initial failure, the Exposure D is 29m/s and the Exposure B is 33m/s. Fig. 6 shows

the comparison of the damage states, and the damage states criteria are shown in Table II [9]. DS 1 is the criterion that 1 out of 480 roof panels is damaged, and DS 4 is the criterion that more than 33% of the 480 roof panels are damaged. It seems reasonable that the higher the DS level, the lower the probability of failure. As a result of checking the probability of failure at a wind velocity of 40 m/s, DS 1 (1 unit failure) was 97.14%, DS 2 (more than 10% failure) was 24.77%, DS 3 (more than 20% failure) was 6.32%, and DS 4 (more than 33% failure) is 1.00%. Fig. 7 compares the pressure resistance coefficient between positive and negative pressure. It can be seen that positive pressure favors the failure of the roof panel and thus increases the probability of survival compared to negative pressure.

Here, the appropriate wind fragility curve was predicted when it was assumed that a serious accident would occur in a NPPs in Korea. Assuming that the surface roughness condition is Exposure C, the wind direction is in the direction parallel to the ridge, which is the direction of the coast, and the damage state is DS 2, which can cause serious accident due to inflow of extreme winds and extreme rain, it is judged to be about DS 2 in Fig. 6.

However, this assumes the specifications of the turbine building. If the specifications of the actual turbine building are applied, it is judged that accurate results can be obtained.

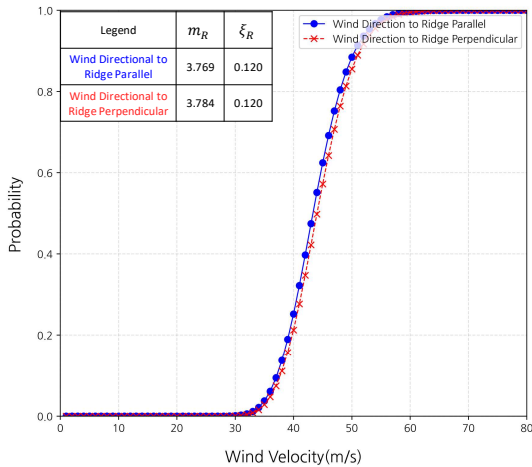


Fig. 4. Fragility Curves Comparing Wind Direction3 (DS 2, Exposure C)

Table II: Damage State (DS)

Damage State	Damage Description	Roof panel Failure
1	Minor Damage	One Panel
2	Moderate Damage	$\geq 10\%$
3	Severe Damage	$\geq 20\%$
4	Destruction	$\geq 33\%$

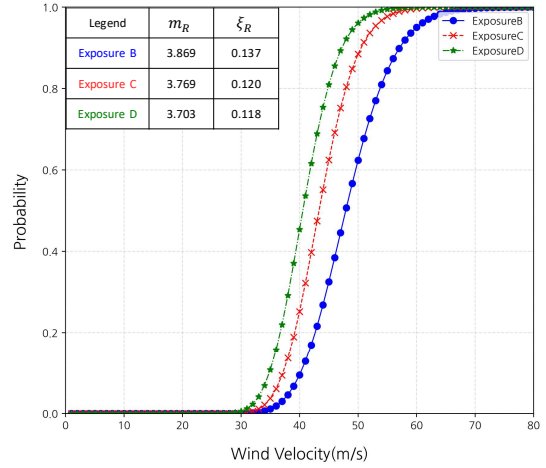


Fig. 5. Fragility Curves Comparing Exposure Types (DS 2, Wind Direction to Ridge Parallel)

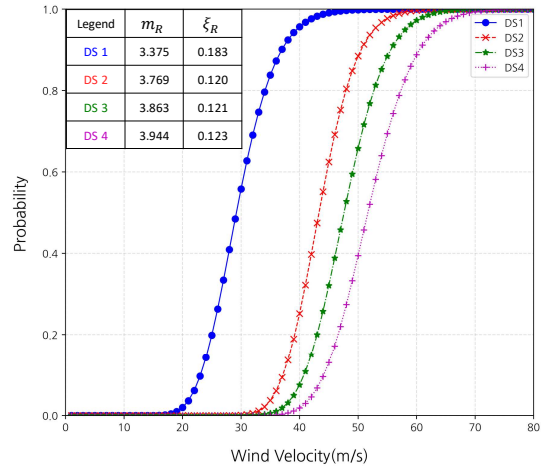


Fig. 6. Fragility Curves Comparing Damage States (Wind Direction to Ridge Parallel, Exposure C)

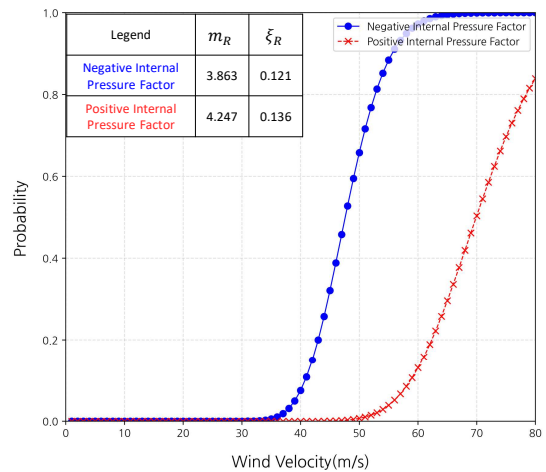


Fig. 7. Fragility Curves Comparing Internal Pressure Factors (DS 3, Wind Direction to Ridge Parallel)

4. Conclusion

In this study, the wind fragility assessment of the roof panel of the turbine building was performed. The specification of roof panel was assumed to be sandwich panel. For wind load calculation, part 3 (a building height of 18 m or more) in components and cladding (chapter 30) presented in ASCE 7-16 were used, and the lognormal cumulative distribution function was converted into a database by applying the MCS algorithm.

As a result of the analysis, it was possible to quantitatively analyze the influence of wind direction, exposure type, damage state, and internal pressure coefficient, and it was possible to confirm the trend.

The limitations of this study were insufficient statistical data related to resistance performance of turbine building and parameters used to calculate wind loads. Also, the damage state criteria of turbine building were not established. For this reason, this study focused on wind fragility assessment methodology for buildings taller than 18 m, such as turbine buildings. In future studies, wind fragility assessment should be conducted by collecting accurate statistical data and establishing criteria for the damage state of turbine building.

ACKNOWLEDGEMENT

This work was supported by the Korea Institute of Energy Technology Evaluation and Planning (KETEP) and the Ministry of Trade, Industry & Energy (MOTIE) of the Republic of Korea (No. 20224B10200040).

REFERENCES

- [1] S. R. Ryu, A Study on the Flooding Risk Assessment of Energy Storage Facilities According to Climate Change, *Journal of The Korean Society of Disaster Information*, Vol. 18, No. 1, pp. 10-18, 2022.
- [2] Korea Hydro & Nuclear Power Co., Ltd., Wolsong Unit 1 Nuclear Power Plant Stress Test performance report (final report), 2013.
- [3] H. G. Jung, S. H. Lee, J. H. Park, and S. D. Kwon, A Study on the Flight Initiation Wind Speed of Wind-Borne Debris, *Journal of Civil and Environmental Engineering Research*, Vol.40, p. 105-110, 2020.
- [4] ASCE, Minimum Design Loads and Associated Criteria for Buildings and Other Structures (ASCE Standard 7-16), American Society of Civil Engineers, 2006.
- [5] B. Baskaran, H. Ham, and W. Lei, New Design Procedure for Wind Uplift Resistance of Architectural Metal Roofing Systems, *Journal of Architectural Engineering*, Vol. 12, p. 168-177, 2006.
- [6] H. J. Ham, S. S. Lee, and H. J. Kim, Development of Extreme Wind Fragility for Lower-rise Industrial Building, *Journal of the Architectural Institute of Korea*, p. 81-88, 2009.

[7] J. K. Choi, and W. Y. Jung, Fragility Evaluation of 154kV Electric Transmission Tower Subjected to Strong Wind, *Journal of the Korean Society for Advanced Composite Structures*, Vol.9, p. 6-14, 2018.

[8] S. S. Lee, H. J. Ham, and H. J. Kim, Fragility Assessment for Cladding of Industrial Buildings Subjected to Extreme Wind, *Journal of Asian Architecture and Building Engineering*, p. 65-72, 2013.

[9] D. Straub, and A. Kiureghian, Improved Seismic Fragility Modeling from Empirical Data, *Structural Safety*, Vol. 30, p. 320-336, 2008.